Heterogeneous & Homogeneous & Bio- & Nano-
CHEMCATCHEM
CATALYSIS

Accepted Article

Title: Pd Catalyzed Surface Reactions Involving H2 of Importance in Radiation Induced Dissolution of Spent Nuclear Fuel

Authors: Annika Carolin Maier and Mats Jonsson

To be cited as: *ChemCatChem* 10.1002/cctc.201901128

Link to VoR: http://dx.doi.org/10.1002/cctc.201901128

A Journal of
ChemPubSoc Europe

WILEY-VCH

www.chemcatchem.org

Pd Catalyzed Surface Reactions Involving H_2 of Importance in Radiation Induced Dissolution of Spent Nuclear Fuel

Annika Carolin Maier*[a] and Mats Jonsson[a]

Abstract: To assess the influence of metallic inclusions (ε-particles) on the dissolution of spent nuclear fuel under deep repository conditions, Pd-catalyzed reactions of H_2O_2, O_2 and UO_2^{2+} with H_2 were studied using Pd-powder suspensions. U(VI) can efficiently be reduced to less soluble U(IV) on Pd-particles in the presence of H_2. The kinetics of the reaction was found to depend on the H_2 partial pressure at $p_{H2} \leq 5.1 \times 10^{-2}$ bar. In comparison, the H_2 pressure dependence for the reduction of H_2O_2 on Pd also becomes evident below 5.1×10^{-2} bar. Surface bound hydroxyl radicals are formed as intermediate species produced during the catalytic decomposition of H_2O_2 on oxide surfaces. While a significant amount of surface bound hydroxyl radicals were scavenged during the catalytic decomposition of H_2O_2 on ZrO_2, no scavenging was observed in the same reaction on Pd. This indicates a different reaction mechanism for H_2O_2 decomposition on Pd compared to metal oxides and is in contrast to current literature. While Pd is an excellent catalyst for the synthesis of H_2O_2 from H_2 and O_2, a similar catalytic activity that was previously proposed for ZrO_2 could not be confirmed.

Introduction

Worldwide around 10 % of the electricity produced today is based on nuclear energy.[1] Although greenhouse gas emissions from nuclear power are low, other waste streams are of particular concern. Most fuel assemblies used in nuclear reactors today are based on UO_2. Used nuclear fuel can be reprocessed, although most countries are currently planning to dispose the highly radioactive used fuel in deep repositories.[2] In case of barrier failure, spent nuclear fuel will be in contact with groundwater. The groundwater at repository sites is expected to be reducing where UO_2 has a very low solubility.[3] However, the inherent radioactivity of the spent nuclear fuel will induce radiolysis of the groundwater in contact with the fuel. As a result, both oxidants ($^{\bullet}OH$, H_2O_2) and reductants (e_{aq}^-, $H^{\bullet}$, H_2) will be produced in the vicinity of the fuel surface.[4] For kinetic reasons, the surface reactions will initially be dominated by the radiolytic oxidants. Under the conditions often used in safety assessments, i.e., groundwater intrusion after more than 1000 years, H_2O_2 has been shown to be the radiolytic oxidant of main importance.[5] The reaction mechanism for oxidative dissolution of UO_2 by H_2O_2 can be described by reactions 1-2.

$$H_2O_2 + UO_{2\,(S)} \rightarrow UO_{2\,ads}^{2+} + 2OH^- \quad (1)$$

$$UO_{2\,ads}^{2+} \rightarrow UO_{2\,dissolved}^{2+} \quad (2)$$

The competing reaction to uranium oxidation is catalytic decomposition of H_2O_2 on the UO_2 surface forming water and molecular oxygen according to reactions 3-5.

$$H_2O_2 \rightarrow 2OH_{ads}^{\cdot} \quad (3)$$

$$OH^{\cdot} + H_2O_2 \rightarrow H_2O + HO_2^{\cdot} \quad (4)$$

$$HO_2^{\cdot} + HO_2^{\cdot} \rightarrow H_2O_2 + O_2 \quad (5)$$

Note the homolytic cleavage of H_2O_2 into surface bound hydroxyl-radicals. Adsorption of the $^{\bullet}OH$ is a prerequisite for this reaction to be spontaneous at room temperature. The ratio between the two competing reactions, H_2O_2 decomposition and uranium dissolution, is often referred to as the dissolution yield (expressed as the ratio between the amount of dissolved uranium and the amount of consumed H_2O_2). The dissolution yield has been found to depend on the H_2O_2 concentration.[6]

When spent nuclear fuel is discarded from a nuclear reactor it consists of around 95 % UO_2, the remaining 5 % being fission products and heavier actinides.[7] Fission products are categorized based on their appearance in spent nuclear fuel according to: 1) Fission gases and volatile fission products, 2) Fission products forming metallic precipitates (ε-particles), 3) fission products forming oxide precipitates as well as 4) fission products which substitute U in the fuel matrix. [8] ε-particles usually contain Mo, Ru, Tc, Rh and Pd in variable ratios depending on the oxygen potential of the fuel and the location from the rim to the center of a fuel pin.[9,10] These metallic particles have been shown to efficiently catalyze several reactions of major importance in the process of radiation-induced dissolution of spent nuclear fuel.[11-15] In

[a] A. C. Maier, Prof. Dr. M. Jonsson
Department of Chemistry
School of Engineering Sciences in Chemistry, Biotechnology and Health
KTH – Royal Institute of Technology
SE-10044 Stockholm, Sweden
E-mail: * acmaier@kth.se

several previous studies on model systems, Pd has been used to mimic the ε-particles,[11, 12] or to reduce U(VI) in order to determine the solubility of UO_2(s).[16,17] Figure 1 summarizes the most important reactions at the interface between spent nuclear fuel and groundwater.

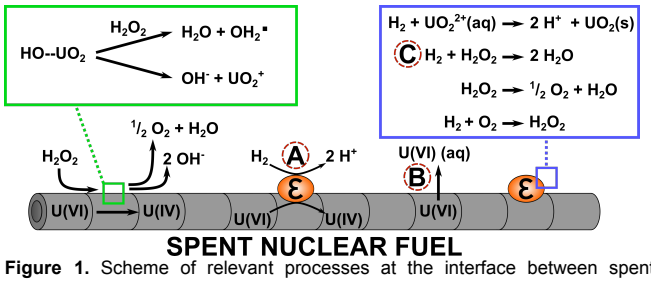

Figure 1. Scheme of relevant processes at the interface between spent nuclear fuel and groundwater.

In a deep repository after barrier failure, reactions catalyzed by metallic inclusions are diverse. The most important processes are the ε-particle catalyzed solid phase reduction of U(VI) to U(IV) (figure 1, reaction A),[15] that efficiently competes with the dissolution of U(VI) (figure 1, reaction B) and the ε-particle catalyzed reaction between H_2O_2 and H_2 (figure 1, reaction C) that reduces the amount of H_2O_2 available for oxidation of the fuel.[11] In addition to being a radiolysis product, H_2 is produced upon anaerobic corrosion of steel.[18] Under deep repository conditions, the hydrogen production rate as a result of canister corrosion was roughly estimated to be in the order of 0.4 mol $year^{-1}$ m^{-2} assuming that 1 mole of hydrogen is produced per mole of consumed metal which leads to a fast buildup of H_2 in the repository.[19]

Studies on simpler model systems have shown that the kinetics of the reaction between H_2O_2 and H_2 catalyzed by Pd is independent of the H_2 partial pressure between 1 bar and 40 bar and that the reaction is virtually diffusion controlled.[11] Under these conditions, the competing catalytic decomposition of H_2O_2 on the Pd particles could not be observed. However, when lowering the H_2 partial pressure sufficiently, the catalytic decomposition of H_2O_2 on the Pd surface will become the predominant reaction pathway. In the literature,[20-22] the reaction mechanism for H_2O_2 decomposition on Pd is claimed to be the same as for metal oxides as described by reactions 3-5, where the surface bound •OH is the key-intermediate.

In addition to the reactions mentioned above, it was previously shown that in the presence of H_2, Pd is a good catalyst to reduce dissolved U(VI) back to U(IV).[12,16,17] The rate of reduction was also found to be independent of the H_2 partial pressure between 1.5 bar and 40 bar.[12] When the same experiment was carried out in the absence of H_2, reduction of U(VI) was not observed. In a recent approach to model the influence of H_2 pressure on the corrosion of fractured spent nuclear fuel, reaction rates for the reduction of uranyl at H_2 pressures below 1.5 bar had to be estimated as experimental results were not available.[23]

To complement missing experimental results for computational models of spent nuclear fuel corrosion in a deep repository, we have performed experiments monitoring the reduction of uranyl as well as H_2O_2 consumption at H_2 partial pressures below 1.5 bar. The partial pressure of H_2 has been varied using gas mixtures containing 100, 5, 0.5, 0.05 and 0 % H_2 in N_2 to make sure that the pressure dependent regime can be identified. To elucidate the mechanism for catalytic decomposition of H_2O_2 on Pd, we used tris(hydroxymethyl)aminomethane (tris) as a scavenger for hydroxyl radicals. The results are compared to results from experiments performed using ZrO_2 instead of Pd. For ZrO_2, the formation of surface bound hydroxyl radicals upon exposure to H_2O_2 has been confirmed and quantified in several studies.[24-26]

Since the beginning of the 20th century it is known that H_2O_2 can form from its elements at ambient temperatures when a suitable catalyst is used.[27] A similar catalytic behavior was recently reported for ZrO_2.[28] In complementary autoclave experiments the H_2O_2 formation from H_2 and O_2 and its successive decomposition on Pd and ZrO_2 was studied, monitoring •OH concentrations over time.

Results and Discussion

Uranyl Reduction by H_2

As can be seen in figure 2, the reduction of U(VI) to U(IV) in the presence of H_2 is catalyzed by Pd. A simplified reaction mechanism is shown in the insert. As mentioned above, it was previously shown that the kinetics of U(VI) reduction shows no dependence on the H_2 partial pressure between 1.5 bar and 40 bar.[12] When decreasing the H_2 partial pressure below 1 bar, it is evident that the reaction rate becomes dependent on the H_2 partial pressure. Compared to the experiments carried out at 1.01 bar H_2, already at 5.1 x 10^{-2} bar H_2 the rate of U(VI)-reduction is decreased by a factor of approximately 2. The largest apparent change in reactivity is observed between 5.1 x 10^{-3} bar and 5.1 x 10^{-4} bar. However, this change can to a large extent be attributed to a difference in the initial lag time of the reaction. The initial lag phase is ascribed to the presence of oxygen in the injected uranyl solution. Its length was found to depend on the H_2 partial pressure. While for 1.01 bar H_2 7 % of the uranyl is reduced after 35 min, only 4 % and 2.5 % respectively is reduced at hydrogen partial pressures of 5.1 x 10^{-3} bar and 5.1 x 10^{-4} bar, during the same time interval. The oxygen concentration can be calculated to be around 14 µM, almost 1.5 times as much as the uranyl present initially. The oxygen in the system is likely to react with H_2 in the

presence of Pd to form H_2O_2. The H_2O_2 in turn can react in several ways among which, one is the re-oxidation of U(IV) to U(VI) or it can react with H_2 to from water. In any case, the reactions involving O_2 / H_2O_2 appear to efficiently compete with the reduction of U(VI) which starts only when the oxidants are consumed.

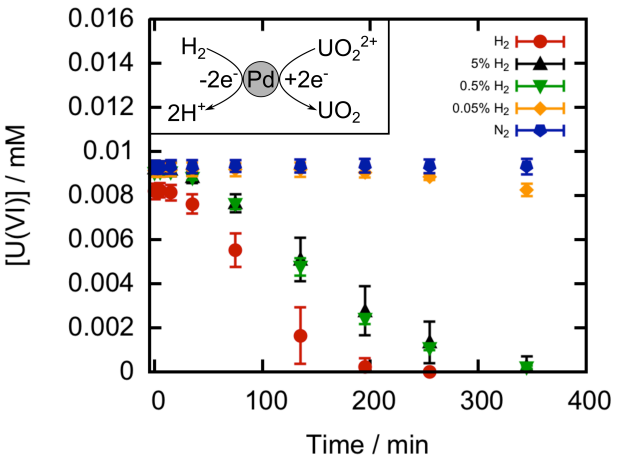

Figure 2. U(VI) reduction as a function of time on 8 mg Pd at different H_2 partial pressures; 1.01 bar H_2 (red dots), 5.1 x 10^{-2} bar H_2 (black triangles), 5.1 x 10^{-3} bar H_2 (green triangles), 5.1 x 10^{-4} bar H_2 (yellow diamonds) and 1.01 bar N_2 (blue diamonds).

H_2O_2 Reactivity

Figure 3 shows the concentrations of H_2O_2 as a function of time in Pd-suspensions in the presence of H_2 and/or N_2. Interestingly, no lag time is observed here even though the H_2O_2 injections also introduce approximately 15 µM O_2 into the system. This is attributed to the initial H_2O_2 concentration being one order of magnitude higher than the expected O_2 concentration, i.e., O_2 and more importantly H_2O_2 formed from O_2 reacting with H_2 can only marginally influence the kinetics for H_2O_2 consumption.

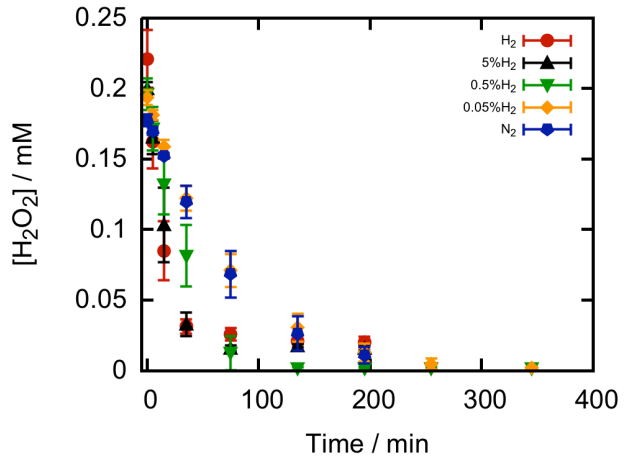

Figure 3. H_2O_2 consumption as a function of time on 8 mg Pd at different H_2 partial pressures; 1.01 bar H_2 (red dots), 5.1 x 10^{-2} bar H_2 (black triangles, 5.1 x 10^{-3} bar H_2 (green triangles), 5.1 x 10^{-4} bar H_2 (yellow diamonds) and 1.01 bar N_2 (blue diamonds).

In table 1 the experimentally determined pseudo-first order rate constants (k_1) for different H_2 partial pressures are given. In contrast to what was observed in a previous study,[11] the reactivity of H_2O_2 is fairly high also in the absence of H_2.

Table 1. Pseudo-first order rate constants for the consumption of H_2O_2 in suspensions containing Pd particles.

H_2 partial pressure / bar	k_1 / s^{-1}	R^2
1.01	(9.3 ± 0.5) x 10^{-4}	0.9945
5.1 x 10^{-2}	(8.8 ± 0.4) x 10^{-4}	0.9963
5.1 x 10^{-3}	(4.32 ± 0.06) x 10^{-4}	0.9997
5.1 x 10^{-4}	(2.198 ± 0.006) x 10^{-4}	0.9999
0.00	(1.91 ± 0.07) x 10^{-4}	0.9974

From table 1, the H_2 pressure dependence becomes evident below 5.1 x 10^{-2} bar. The background consumption of H_2O_2 on the glass vessel as well as the dissolution of Pd species (determined by ICP-OES) are negligibly small during the timeframe of the experiments.

As can be seen, the overall reactivity of H_2O_2 decreases with decreasing H_2 partial pressure. The consumption of H_2O_2 displays first order kinetics for a given H_2 partial pressure (k_1 vs. p_{H2} is shown in figure 4a). Hence, the rate-determining step is the reaction between H_2O_2 and Pd (reaction (6)), and adsorption of H_2 (reaction (7)) is fast enough to keep the level of adsorbed H_2 constant.

$$H_2O_2 + Pd \cdots H_{ads} \rightarrow Products \quad (6)$$

$$H_2 \xrightarrow{Pd} Pd \cdots H_{ads} \quad (7)$$

The rate law for H_2O_2 consumption through Pd catalyzed reduction by H_2 can then be described according to equation 8,

$$-\frac{d[H_2O_2]}{dt} = k\,[H_2O_2]\theta \quad (8)$$

where Θ is the fractional surface coverage of H_2 on the Pd particles. Equation 8 can be simplified to equation 9 if the concentration of adsorbed H_2 on the Pd-particles is considered to be constant (k^* = kΘ).

$$\frac{d[H_2O_2]}{dt} = -k^*\,[H_2O_2] \quad (9)$$

Hence, we expect to observe first order kinetics. Note that k^*

is k_1-k_{cat}, i.e. the observed rate constant minus the rate constant for the catalytic decomposition of H_2O_2 on Pd. From the experiments we have determined k^* at different H_2 partial pressures i.e. at different Θ. Assuming that Θ can be described by the Langmuir isotherm, we can express k^* through equation 10.

$$k^* = \frac{k\,K\,[H_2]}{K\,[H_2]+1} \quad (10)$$

Inverting equation 10 gives a linear relationship (equation 11).

$$\frac{1}{k^*} = \frac{1}{k} + \frac{1}{kK[H_2]} \quad (11)$$

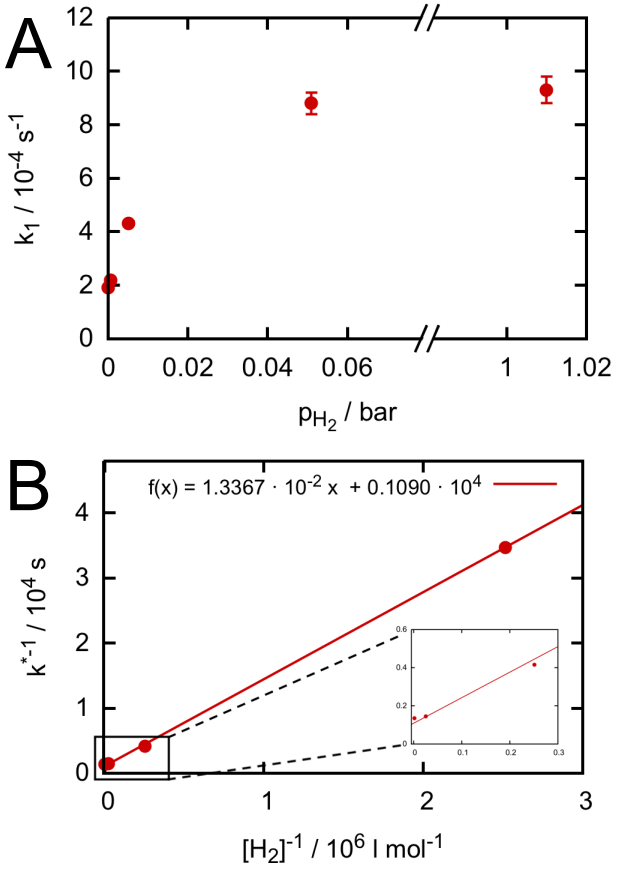

Figure 4. (A) First order rate constants for H_2O_2 consumption at different p_{H2} and (B) a Langmuir Hinshelwood plot for the kinetics of H_2O_2 consumption.

When plotting the experimental data using equation 11 (figure 4b) one obtains an intercept of 1.09 x 10^3 s and a slope of 1.34 x 10^{-2} s M. From the intercept the second order rate constant, k, can be calculated to 9.2 x 10^{-4} s^{-1}. From the slope of figure 4b and the rate constant, the equilibrium constant for adsorption of H_2 can be calculated to 8.1 x 10^4 M^{-1}.

The rate constant determined above is only valid at the solid surface area to solution volume ratio used in the experiments. In a previous study, the kinetics of H_2O_2 consumption was studied as a function of Pd surface area to solution volume ratio at H_2 pressures above 1 bar. [11] Under these conditions the rate of H_2O_2 consumption is independent of the H_2 pressure, i.e. θ =1. The rate expression under these conditions can be written as follows (equation 12):

$$-\frac{d[H_2O_2]}{dt} = k_2[H_2O_2] \cdot \frac{SA}{V} \quad (12)$$

and the rate constant k_2 was determined to 2.2 x 10^{-5} m s^{-1}. In the present study we can estimate the corresponding H_2 pressure independent rate constant to 2.4 x 10^{-5} m s^{-1}. The perfect agreement between the two results is mainly coincidental, as two different batches of Pd-particles were used and the specific surface area in the work by Nilsson and Jonsson was estimated from the average Pd-particle size. To obtain a rate expression that is valid at all H_2 pressures we can combine the two expressions to equation 13,

$$-\frac{d[H_2O_2]}{dt} = k_2\,[H_2O_2] \cdot \frac{SA}{V} \cdot \theta \quad (13)$$

where k_2 = 2.4 x 10^{-5} m s^{-1}. In comparison, the second order rate constant for a diffusion controlled process when µm-sized particle suspensions are used is in the order of 10^{-3} m s^{-1}.[29] Hence, the reactions studied here are clearly not diffusion controlled.

Interestingly, when the system is purged and stirred for a longer time before the injection of H_2O_2 (i.e. for 16 h instead of 30 min), the reactivity of H_2O_2 towards Pd is significantly decreased. This is illustrated for N_2 purged samples in figure 5. A similar decrease in reactivity was observed in uranyl reduction experiments, when the stirring and purging time was increased before the uranyl injection (data not shown).

Particle agglomeration is known to be a common phenomenon decreasing the catalytic activity of Pd by reducing the available surface area.[30] SEM images of the Pd powder after different time intervals during which the powder suspensions were stirred are shown in figure 6. From the images, an increase in agglomerate size can be observed, to which we qualitatively ascribe its reduced reactivity. This observation connects the higher reactivities from this work, with previously published results where significantly lower reactivities were observed.[11,12] It should be noted that the Pd-suspensions in the work by Nilsson and Jonsson [11,12] were continuously stirred in an autoclave over night before the injection of uranyl or H_2O_2 respectively.

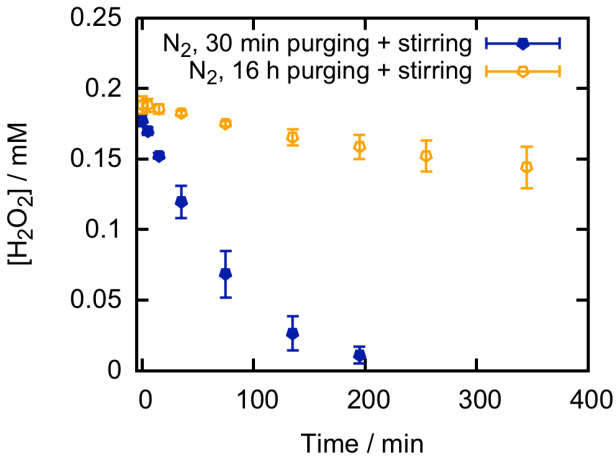

Figure 5. H_2O_2 consumption as a function of time on 8 mg Pd and N_2 purging. Purging and stirring for 30 min before the H_2O_2 injection (filled blue pentagons), as well as purging and stirring for 16 h before the H_2O_2 injection (open orange pentagons).

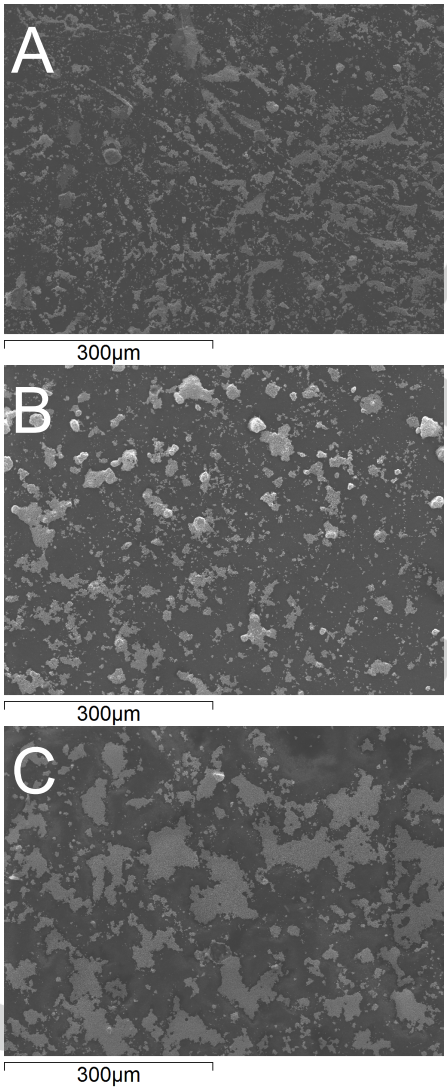

Figure 6. SE-SEM images of Pd-powder that was exposed to water without stirring and purging (A), Pd powder that was stirred and purged for 30min before the injection of H_2O_2 (total stirring time approx. 6 h)(B) and Pd powder that was stirred and purged for 16 h before the injection of H_2O_2 (total stirring time approx. 22 h)(C).

From the results presented above it is obvious that H_2O_2 is catalytically decomposed on the Pd surface. When comparing the reactivity of H_2O_2 towards ZrO_2 and Pd in the presence of tris as scavenger for surface bound $^{\bullet}OH$ (figure 7a), it is clear that the reactivity of H_2O_2 towards untreated Pd powder is higher as compared to ZrO_2. It should be noted that the solid surface area to solution volume ratio is a factor of 10 higher in the case of ZrO_2 in the experiment and therefore the difference in reactivity between ZrO_2 and Pd is even larger than it appears in figure 7a. Experiments performed on ZrO_2 in the presence of tris as $^{\bullet}OH$ scavenger show that there is a significant production of CH_2O (the final product in the reaction between $^{\bullet}OH$ and tris) when H_2O_2 is consumed (figure 7b). Since the yield of formaldehyde is proportional to the concentration of surface bound $^{\bullet}OH$, tris can be used as a quantitative probe for $^{\bullet}OH$. A reaction mechanism for the reaction between $^{\bullet}OH_{ads}$ and tris was proposed by Yang and Jonsson.[31]

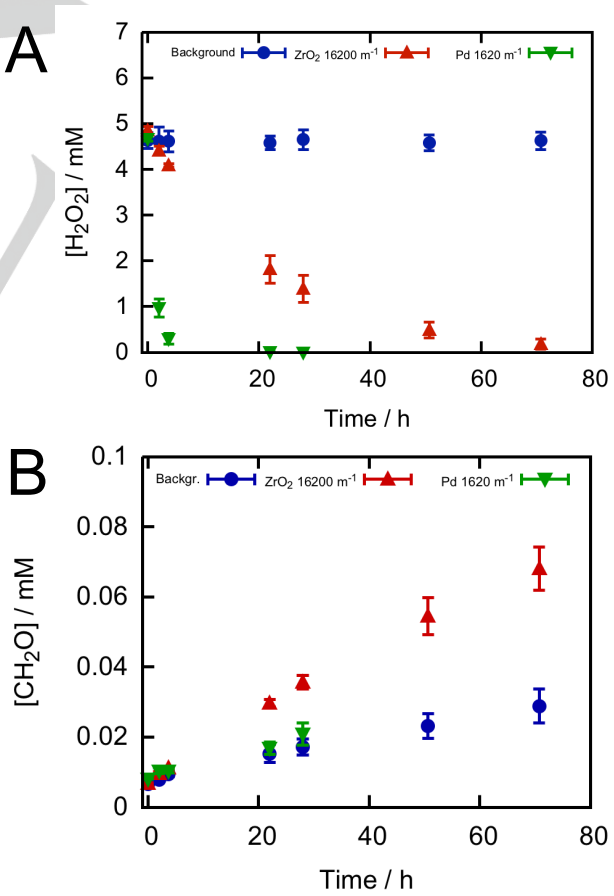

Figure 7. (A) H_2O_2 decomposition and (B) CH_2O production from scavenged $^{\bullet}OH$ over time with SA/V = 1620 m^{-1} for Pd (green triangles down) and 16200

m^{-1} for ZrO_2 (red triangles).

The final yield of formaldehyde depends on the relative surface coverage of both adsorbed H_2O_2 and tris (governed by their initial concentrations and the relative affinity of the adsorbent to the surface) as well as the competition for $^{\bullet}OH$ by H_2O_2 and tris.[26]

It is interesting to note that, even though H_2O_2 reacts rapidly with Pd, no CH_2O above background levels can be detected. This implies that no significant amount of scavengeable $^{\bullet}OH$ is formed upon catalytic decomposition of H_2O_2 on the Pd surface. Consequently, the mechanism of catalytic decomposition of H_2O_2 on Pd would appear to differ from that of H_2O_2 on ZrO_2. This finding contradicts the assumption made in the literature [20-22] that the reaction mechanism for H_2O_2 decomposition on the Pd surface is the same as on metal oxides (reactions 3-5). A reaction mechanism, which does not include the $^{\bullet}OH$, was to the best of our knowledge only proposed in the 1960s,[32-34] but was rarely considered in later research.

Autoclave Experiments

To further explore the activity of Pd as a model for ε-particles in catalyzing reactions between molecular radiolysis products, we studied the formation (reaction 14) and subsequent decomposition of H_2O_2 in an autoclave originally containing H_2 and O_2 in contact with an aqueous suspension containing Pd particles. The results are shown in figure 8.

$$H_2 + O_2 \xrightarrow{Pd} H_2O_2 \qquad (14)$$

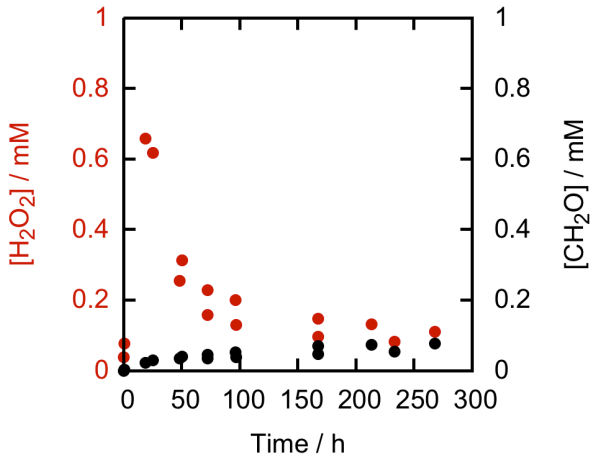

Figure 8. H_2O_2 production and consecutive consumption on Pd at p_{H2} = 40 bar and p_{O2} = 0.2 bar. The displayed data points are the result of two identical experiments to assure reproducibility.

Based on the volume of the autoclave and the oxygen concentration in air, a theoretical H_2O_2 concentration of 190 mM could be reached in the reaction vessel, assuming that all O_2 is dissolved and converted into H_2O_2. Due to the continuous and rapid consumption of H_2O_2 on Pd as well as the time interval for sampling, the measured peak concentration of approximately 0.7 mM H_2O_2, is well below the theoretical maximum.

When measuring CH_2O over time, it is evident that the concentration hardly increases. The slight increase is most likely due to scavenging of $^{\bullet}OH$ produced in the background decomposition of H_2O_2. As in the experiment described above (addition of H_2O_2 to a Pd-suspension), this result shows that hydrogen-abstracting radicals (like the $^{\bullet}OH$), which could lead to a significant production of CH_2O, are not produced in the system.

Results from autoclave experiments where ZrO_2 was used to catalyze the reaction between O_2 and H_2 (in the absence of Pd) are shown in figure 9. Note that the detection limit for H_2O_2 is approx. 0.01 mM. As can be seen, there is no detectable H_2O_2–formation (figure 9a), which indicates that H_2O_2 is either not produced at all, or it rapidly decomposes on the surface of ZrO_2. The latter would result in the formation of CH_2O. As can be seen, the CH_2O concentration increases significantly in the presence of ZrO_2 (red triangles pointing downwards) when a PEEK (Polyether ether ketone) stirrer is used. However, using the same stirrer in the absence of ZrO_2, the background production of CH_2O (blue dots) overlaps the results for ZrO_2 within the uncertainty of the experiment.

In a previous study based on experiments using the same equipment a very similar observation was made in the presence of ZrO_2.[28] In this case the CH_2O concentration reached approximately 225 µM after 300 h. This concentration is only slightly higher compared to the results presented above. From the previous results (where also H_2O_2 was detected as a transient)[28] it was concluded, that ZrO_2 catalyzes the reaction between H_2 and O_2 to form H_2O_2. However, in that study background measurements were never made as PEEK was assumed to be an inert material. When removing the stirrer and in the absence of any powder, neither H_2O_2 nor CH_2O are produced in detectable quantities (Figure 9b orange triangles). The same was found in the presence of ZrO_2 when the PEEK stirrer was replaced with a glass stirrer (Figure 9b green diamonds). As neither, H_2O_2 nor CH_2O are detectable in concentrations above background, we must ascribe the catalytic activity that was reported in [28] to aging of the PEEK stirrer or a contamination with Pd. We found that 2 mg of Pd is enough to produce a significant amount of H_2O_2 (figure 8). As Pd was previously used in the same autoclave,[11,12] small quantities could have contaminated the stirrer still being enough to see the enhanced background in the presence of the PEEK stirrer.

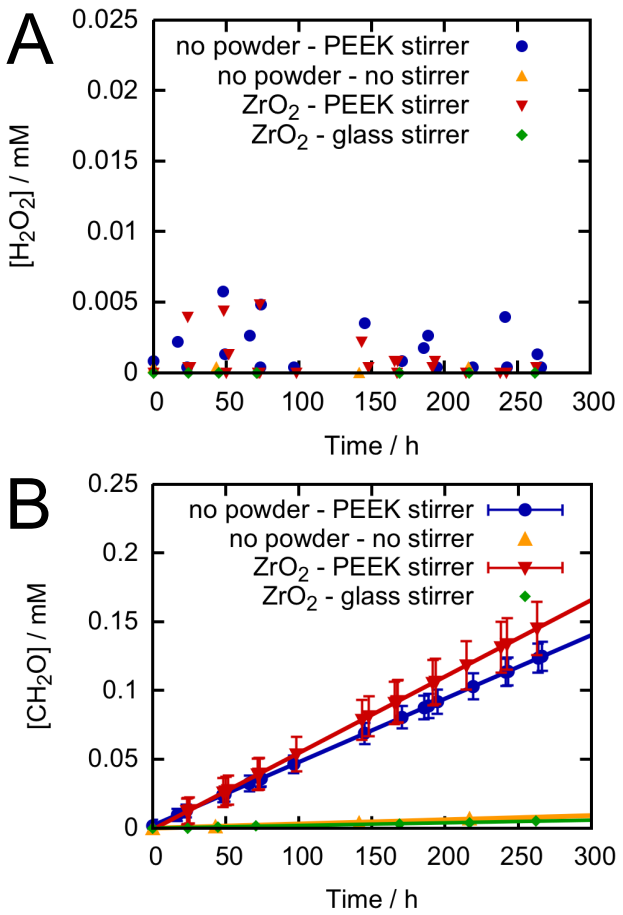

Figure 9. (A) H_2O_2 and (B) CH_2O concentrations measured over time in the absence of Pd at p_{H2} = 40 bar and p_{O2} = 0.3 bar.

Conclusions

The experimental results presented above give new insights on the effects of ε-particle (mimicked by Pd) catalyzed reactions in a deep geological repository. In case of groundwater intrusion into a repository, ε-particles can efficiently reduce dissolved U(VI) to the considerably less soluble U(IV), even in the presence of small quantities of H_2. The reduction of U(VI) was found to become depended on the H_2 partial pressure at $p_{H2} \leq 5.1 \times 10^{-2}$ bar. The reactivity of H_2O_2, the key radiolysis product to induce oxidative dissolution also decreases with decreasing H_2 partial pressure, where the dependence also becomes evident below 5.1×10^{-2} bar. We found that formaldehyde is not produced in the reaction between H_2O_2 and Pd in the presence of tris, which indicates that •OH is not formed during catalytic decomposition of H_2O_2 on Pd. In contrast, a significant amount of hydroxyl radicals are scavenged in the same reaction on ZrO_2. The absence of •OH during H_2O_2 decomposition on Pd indicates that the reaction mechanism, which is proposed in current literature, needs to be revised. Compared to previous results, where ZrO_2 was shown to catalyze the reaction between H_2 and O_2 to form H_2O_2, we were not able observe the same catalytic behavior ascribing the catalytic behavior reported earlier to contamination or aging of the experimental setup.

Experimental Section

ZrO_2 as well as Pd powder used during the experiments are listed in Table 1 and were used as received. The BET surface area of ZrO_2 was determined by isothermal adsorption and desorption of a 30 % N_2 in He gas mixture on a Micrometrics Flowsorb II 2300 device. For Pd, the specific surface area was calculated from the particle sizes given by the supplier. Throughout all experiments purified water (18.2 MΩ cm, Merck MilliQ) was used.

Table 1. Powders used during the experiments

Metal / Metal Oxide	Supplier	Specific Surface Area / $m^2\ g^{-1}$
ZrO_2	Aldrich 99 %	6.44 ± 0.05
Pd	Aldrich ≥ 99.9 %	1.35 calculated

Uranium concentrations were measured spectrophotometrically at 653 nm using the Arsenazo III method [35], whereas H_2O_2 concentrations were measured using the Ghormley triiodide method [36]. U(VI) in solution absorbs light at the low wavelength side of the triiodide peak at 350 nm. To avoid an overlap of the two peaks, samples containing uranium were therefore measured at 360 nm instead. Individual calibrations were made for both wavelengths.

Hydroxyl radicals were scavenged using tris (BDH chemicals ≥ 99 %). Tris reacts with hydrogen abstracting radicals to form formaldehyde, which can be measured indirectly by spectrophotometry using the modified Hantzsch method [37]. Samples containing formaldehyde were left to react with 2 M ammonium acetate (Sigma Aldrich ≥ 99 %) and 0.04 M acetoacetanilide (SAFC, Sigma Aldrich ≥ 98 %) for 15 min at 40 °C forming a dihydropyridine derivative, which can be measured at 368 nm. Before each experiment with tris, the pH was adjusted to 7.5 with HCl.

Experiments on aqueous powder suspensions where the partial pressure of H_2 was varied, were carried out in a three neck round bottom flask. One of the necks was permanently closed with a glass stopper, the second one with a septum and a custom made in-/outlet for purging and sampling was inserted into the third neck. The in- and outlet is equipped with two valves and a glass frit for purging. When closing the valve that is used to release excess gas, the vessel can temporarily be slightly pressurized. The overpressure in the vessel is then used to drive a liquid sample up through the glass frit from where it can be released through the second valve. After sampling, the overpressure was quickly released back to 1 atm. By using the custom made in-/outlet the aqueous powder suspensions could be continuously purged with pre-mixed gases (Table 2) without

air intrusion during sampling. In the absence of H_2, the samples were purged throughout the experiment using N_2.

Table 2. Overview of gases used during the experiments

H_2 partial pressure / %	H_2 partial pressure / bar	Purity / %
100	1.01	≥ 99.995
5	5.1×10^{-2}	
0.5	5.1×10^{-3}	
0.05	5.1×10^{-4}	
0 (100 % N_2)	0.00	≥ 99.999

Uranyl reduction by H_2

To measure the kinetics of UO_2^{2+} reduction depending on the H_2 partial pressure below 1 bar, different gas mixtures were used (table 2). 8 mg of Pd were suspended in HCO_3^- solution and the mixture was deoxygenized through purging for 30 min in the custom made setup as described above. The gas flow was kept constant at 0.9 l min^{-1} and the sample was stirred using a magnetic stirrer throughout the experiment.

After the 30 min equilibration time, 0.56 ml 5 mM uranyl nitrate were injected into the reaction vessel through the septum using a hypodermic needle to reach a total volume of 280 ml, a HCO_3^- concentration of 2 mM and a uranyl concentration of 0.01 mM. U(VI) concentrations were measured over time.

H_2O_2 reactivity as a function of the H_2 partial pressure

To determine the reactivity of H_2O_2 towards H_2 on Pd, H_2O_2 concentrations were measured over time as a function of H_2 partial pressure below 1 bar. 8 mg of Pd powder were suspended in water and the mixture was left to deoxygenize through purging for 30 min. After this equilibration time H_2O_2 was injected through the septum into the reaction vessel using a hypodermic needle to a total volume of 280 ml and a H_2O_2 concentration of 0.22 mM. The gas flow was kept constant at 0.9 l min^{-1} and the sample was stirred using a magnetic stirrer throughout the experiment. H_2O_2 concentrations were measured over time.

Catalytic decomposition of H_2O_2

For experiments where the production of surface bound $^{\bullet}OH$ was measured simultaneously to H_2O_2 decomposition, 30 mg of Pd powder were added to a 20 mM tris solution and the pH was adjusted to 7.5 using HCl. The mixture was purged with N_2 to deoxygenize for 30 min and H_2O_2 was added to a concentration of 5 mM and a total volume of 25 ml. As a comparison to the Pd case, the same experiment was performed using 63 mg of ZrO_2 powder instead of Pd. The background consumption of H_2O_2 was determined in the absence of any powder. All samples were stirred using a magnetic stirrer, purged with N_2 and protected from light throughout the experiment. H_2O_2 as well as CH_2O concentrations were measured over time.

Autoclave experiments

For the autoclave experiments 2 mg of Pd, or 2.33 g of ZrO_2 were suspended in 100 ml 20 mM Tris. As for the previous experiments the pH was adjusted to 7.5 with HCl before the reaction vessel was transferred into an aerated autoclave. The autoclave was then pressurized with H_2 to give final partial pressures of 0.2 bar O_2 and 40 bar H_2. Throughout the experiments the powder suspensions were stirred with a paddle stirrer to avoid sedimentation. Samples were taken during two weeks and the concentrations of H_2O_2 as well as $^{\bullet}OH$ were monitored.

Acknowledgements

The Swedish Nuclear and Fuel Waste Management Company (SKB) is gratefully acknowledged for financial support.

Keywords: ε-particles • heterogeneous catalysis • hydrogen • palladium • spent nuclear fuel

[1] IAEA, Energy, electricity and nuclear power estimates for the period up to 2050, IAEA-RDS-1/38, **2018**.

[2] B. Faybishenko, J. Birkholzer, D. Sassani, P. Swift, Eds., International Approaches for Deep Geologic Disposal of Nuclear Waste: Geological Challenges in Radioactive Waste Isolation, Fifth World Wide Review, LBNL Report 1006984, Lawrence Berkeley National Laboratory, Sandia National Laboratories, University of California, Berkeley, USA, **2016**, https://doi.org/10.2172/1353043.

[3] A.S. Kertes, R. Guillaumont, *Nuclear and Chemical Waste Menagement* **1985**, *5*, 215-219.

[4] J. W. T. Spinks, R. J. Woods, An Introduction to Radiation Chemistry, third ed., John Wiley and Sons Inc., New York. **1990**.

[5] E. Ekeroth, O. Roth, M. Jonsson, *J. Nucl. Mater.* **2006**, *355*, 38-46.

[6] A. Barreiro Fidalgo, Y. Kumagai, M. Jonsson, *J. Coord. Chem.* **2018**, *71*, 1799-1807.

[7] J. Bruno, R.C. Ewing, *Elements* **2006**, *2*, 343-349.

[8] H. Kleykamp, *J. Nucl. Mater.* **1985**, *131*, 221-246.

[9] H. Kleykamp, J.O. Paschoal, R. Pejsa, F. Thümmler, *J. Nucl. Mater.* **1985**, *130*, 426-433.

[10] D. Cui, J. Low, C.J. Sjöstedt, K. Spahiu, *Radiochim. Acta* **2004**, *92*, 551-555.

[11] S. Nilsson, M. Jonsson, *J. Nucl. Mater.* **2008**, *372*, 160-163.

[12] S. Nilsson, M. Jonsson, *J. Nucl. Mater.* **2008**, *374*, 290-292.

[13] M. Jonsson, F. Nielsen, O. Roth, E. Ekeroth, S. Nilsson, M.M. Hossain, *Environ. Sci. Technol.* **2007**, *41*, 7087-7093.

[14] M. Trummer, M. Jonsson, *J. Nucl. Mater.* **2010**, *396*, 163-169.

[15] M.E. Broczkowski, J.J. Noël, D.W. Shoesmith, *J. Nucl. Mater.* **2005**, *346*, 16-23.

[16] J. Bruno, I. Grenthe, B. Lagerman, *Mat. Res. Soc. Symp. Proc.* **1985**, *50*, 299-308.

[17] J. Bruno, I. Casas, B. Lagerman, M. Munoz, *Mat. Res. Soc. Symp. Proc.* **1986**, *84*, 152-160.

[18] J.P. Simpson, R. Schenk, B. Knecht, *Mat. Res. Soc. Symp. Proc.* **1985**, *50*, 429-436.

[19] B. Bonin, M. Colin, A. Dutfoy, *J. Nucl. Mater.* **2000**, *281*, 1-14.

[20] J. Li, A. Staykov, T. Ishihara, K. Yoshizawa, *J. Phys. Chem. C.* **2011**, *115*, 7392-7398.

[21] A. Plauck, E. E. Stangland, J. A. Dumesic, M. Mavrikakis, *Proc. Natl. Acad. Sci. U.S.A.* **2016**, *113*, E1973-E1982.

[22] N.M. Wilson, D.W. Flahety, *J. Am. Chem. Soc.* **2016**, *138*, 574-586.

[23] N. Liu, L. Wu, Z. Qin, D.W. Shoesmith, *Environ. Sci. Technol.* **2016**, *50*, 12348-12355.

[24] C.M. Lousada, M. Jonsson, *J. Phys. Chem. C* **2010**, *114*, 11202-11208.

[25] C.M. Lousada, A.J. Johansson, T. Brink, M. Jonsson, *J. Phys. Chem. C* **2012**, *116*, 9533-9543.

[26] M. Yang, M. Jonsson, *J. Mol. Catal. Chem.* **2015**, *400*, 49-55.

[27] H. Henkel, W. Weber, US Patent No. 1108752A, **1914**.

[28] A. Barreiro Fidalgo, B. Dahlgren, T. Brinck, M. Jonsson, *J. Phys. Chem. C* **2016**, *120*, 1609-1614.

[29] M. Jonsson in *Recent Trends in Radiation Chemistry* (Eds.: J. F. Wishart, B. S. M. Rao), World Scientific Publishing Co. Pte. Ltd., Singapore, **2010**, pp. 301-323.

[30] P. Albers, J. Pietsch, S.F. Parker, *J. Mol. Catal. Chem.* **2001**, *173*, 275-286.

[31] M. Yang, M. Jonsson, *J. Phys. Chem. C* **2014**, *118*, 7971-*7979*.

[32] T. A. Pospelova, N. I. Kobozev, E. N. Eremin, *Rus. J. Phys. Chem. Trans.* **1961**, *35*, 299-305.

[33] T. A. Pospelova, N. I. Kobozev, *Rus. J. Phys. Chem. Trans.* **1961**, *35*, 535-542.

[34] T. A. Pospelova, N. I. Kobozev, *Rus. J. Phys. Chem. Trans.* **1961**, *35*, 1192-1197.

[35] S. B. Savvin, Talanta **1961**, *8*, 637-685.

[36] A. O. Allen, T. W. Davis, G.V. Elmore, J. A. Ghormley B. M. Haines, C. J. Hochanadel, ORNL Publications 130, Oak Ridge National Laboratory, Tennessee, USA, **1949**.

[37] Q. Li, P. Sritharathikhun, S. Motomizu, *Anal. Sci.* **2007**, *23*, 413-417.

10.1002/cctc.201901128

WILEY-VCH

Entry for the Table of Contents

FULL PAPER

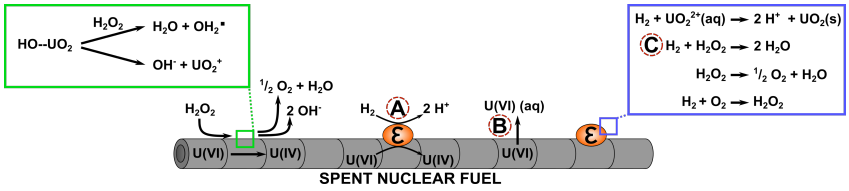

Annika Carolin Maier, Mats Jonsson*

Page No. – Page No.

Pd Catalyzed Surface Reactions involving H_2 of Importance in Radiation Induced Dissolution of Spent Nuclear Fuel

Pd catalyzes UO_2^{2+} and H_2O_2 reduction even at low H_2 partial pressures. Catalytic decomposition of H_2O_2 on Pd has a different mechanism than on metal oxides. While Pd catalyzes H_2O_2 formation from its elements, the same catalytic activity that was proposed for ZrO_2 could not be confirmed.